Dyes and Pigments 91 (2011) 481–488

Contents lists available at ScienceDirect

Dyes and Pigments

journal homepage: www.elsevier.com/locate/dyepig

Synthesis and photophysical properties of structural isomers of novel 2,10-disubstituted benzofuro[2,3-*e*]naphthoxazole-type fluorescent dyes

Haruka Egawa Ooyama [a,*], Yousuke Ooyama [b], Toshihiko Hino [a], Takehiro Sakamoto [a], Takahiro Yamaguchi [b], Katsuhira Yoshida [a,b,*]

[a] Department of Applied Science, Graduate School of Integrated Arts and Science, Kochi University, Akebono-cho, Kochi 780-8520, Japan
[b] Department of Applied Science, Faculty of Science, Kochi University, Japan

ARTICLE INFO

Article history:
Received 10 December 2010
Received in revised form
26 March 2011
Accepted 30 March 2011
Available online 13 April 2011

Keywords:
Fluorescent dye
Photophysical property
Substituent effect
Solid-state fluorescence
Crystal structure
Structual isomers

ABSTRACT

Structural isomers of novel 2,10-disubstituted benzofuro[2,3-*e*]naphthoxazole fluorescent dyes have been synthesized. The phtophysical properties have been investigated in solution and in the solid state. The absorption and fluorescence intensities of the naphth[1,2-*d*]oxazoles are much stronger than those of the naphth[2,1-*d*]oxazoles in solution. Moreover, in the solid state, the emission intensities of the former are typically much stronger than those of latter isomers. To understand the differences in photophysical properties, semi-empirical molecular orbital calculations and the X-ray crystallographic analyses have been performed.

1. Introduction

Benzoxazole derivatives have received considerable attention because of important applications as laser dyes, organic scintillators, and UV dyes in the optoelectronic industry [1–4] and as antibacterial agents, HIV protease inhibitors, and antitumor agents in medicine [5–9]. In particular, intense absorption and emission properties of benzooxazole-type dyes are very useful as organic sensitizers for dye-sensitized solar cells and as emitters for organic electroluminescence devices [10–15]. Recently, Ooyama *et al.* have reported that a novel asymmetric heterocyclic *o*-quinone, 3-dibutylamino-8*H*-5-oxa-8-aza-indeno[2,1-*c*]fluorene-6,7-dione was allowed to react with *p*-cyanobenzaldehyde to give the structural isomers of the novel benzofuro[2,3-*c*]oxazolo[4,5-*a*] carbazole-type (**1**) and benzofuro[2,3-*c*]oxazolo[5,4-*a*]carbazole-type (**2**) fluorophores which differ in the position of oxygen and nitrogen atoms of the oxazole ring (Fig. 1) [16,17]. In a previous study, we reported the novel asymmetric heterocyclic *o*-quinones, 9-dibutylaminobenzo[*b*]naphtho[1,2-*d*]furan-5,6-dione (**3**) can be prepared by the reaction of sodium 1,2-naphthoquinone-4-sulphonate with *m*-dibutylaminophenol [18]. In this present study, we designed and synthesized the structural isomers of novel 2,10-disubstituted benzofuro[2,3-*e*]naphth [1,2-*d*]oxazole-type (**4**) and 2,10-disubstituted benzofuro[2,3-*e*]naphth[2,1-*d*]oxazole-type (**5**) fluorophores with various substituents conjugated to the chromophore skeletons which were derived from the condensation reaction of **3** with various arylaldehydes in the presence of ammonium acetate as the nitrogen source. The photophysical properties of these isomers **4** and **5** in solution and in the crystalline state were investigated. To understand the differences in photophysical properties between the structural isomers and the dramatic substituent effects on the photophysical properties, semi-empirical molecular orbital calculations (AM1 and INDO/S) and X-ray crystallographic analyses were performed. On the basis of these results, relationships between the observed photophysical properties and the chemical and crystal structures of these isomeric fluorophores are discussed.

2. Experimental

Melting points were determined on Rigaku Thermo Plus 2 system TG8120. IR spectra were recorded on a JASCO FT/IR-5300 spectrometer for sample in KBr pellet form. Absorption spectra were observed with a JASCO UV-670 spectrophotometer and

* Corresponding authors. Tel.: +81 88844 8296; fax: +81 88844 8359.
E-mail address: kyoshida@kochi-u.ac.jp (K. Yoshida).

0143-7208/$ – see front matter © 2011 Elsevier Ltd. All rights reserved.
doi:10.1016/j.dyepig.2011.03.031

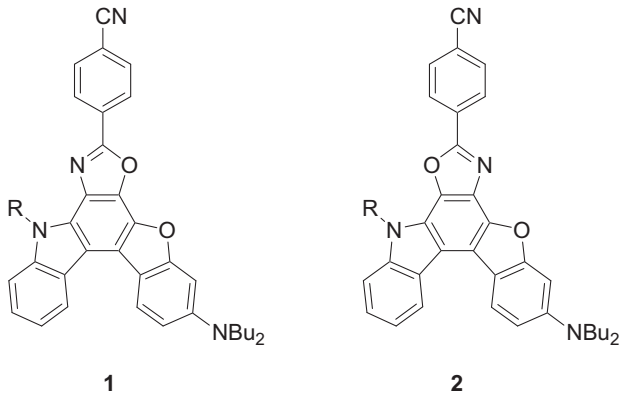

Fig. 1. Ooyama et al. have reported novel benzofuro[2,3-*c*]oxazolo[4,5-*a*] carbazole-type (1) and benzofuro[2,3-*c*]oxazolo[5,4-*a*]carbazole-type (2) fluorophores.

fluorescence spectra were measured with a JASCO FP-6600 spectrophotometer. The fluorescence quantum yields (Φ) of solutions and the crystals were determined by a Hamamatsu C9920-12 by using a calibrated integrating sphere. Elemental analyses were recorded on a Perkin Elmer 2400 II CHN analyzer. ^{1}H and ^{13}C NMR spectra were recorded on a JNM-LA-400 (400, 100 MHz) FT NMR spectrometer with tetramethylsilane (TMS) as an internal standard. Column chromatography was performed on silica gel (KANTO CHEMICAL, 60N, spherical, neutral).

2-(4-carboxyphenyl)-10-dibutylamino-benzofuro[2,3-*e*]naphth [1,2-*d*]oxazole (4a') and 2-(4-carboxy phenyl)-10-dibutylamino-benzofuro[2,3-*e*]naphth[2,1-*d*]oxazole (5a'): A solution of 3 (2.00 g, 5.32 mmol), *p*-carboxybenzaldehyde (0.96 g, 6.38 mmol), and ammonium acetate (8.22 g, 107 mmol) in acetic acid (30 mL) was stirred at 90 °C for 1 h. The reaction mixture poured into cold water, causing the precipitate and then filtered. The resulting residue was washed with CH_2Cl_2 to give the mixture of 4b' and 5b' (2.67 g, quant.) as a yellow powder which was used directly in subsequent reactions.

2-(4-butoxycarbonylphenyl)-10-dibutylamino-benzofuro[2,3-*e*] naphth[1,2-*d*]oxazole **(4a)** and 2-(4-butoxycarbonylphenyl)-10-dibutylamino-benzofuro[2,3-*e*]naphth[2,1-*d*]oxazole **(5a)**: A solution of the mixture of 4a' and 5a' (0.40 g, 0.79 mmol), butyl iodide (0.27 g, 1.48 mmol), and Na_2CO_3 (0.20 g, 1.87 mmol) in DMF (20 mL) was stirred at 100 °C for 10 h. The reaction mixture poured into cold water, causing the precipitate and then filtered. The resulting residue was extracted with CH_2Cl_2, and washed with water. The organic extract was evaporated. The residue was chromatographed on silica gel (toluene : acetic acid = 10 : 1 as eluent) to give 4a (0.37 g, yield 84%) as a yellow powder and 5a (0.03 g, yield 1%) as a yellow powder.

Compound **4a:** M.p. 176.6 °C; ^{1}H NMR (400 MHz, [D_3]chloroform, TMS): δ = 0.99–1.04 (m, 9H), 1.44 (tq, 4H), 1.53 (tq, 4H), 1.68 (tt, 2H), 1.81 (tt, 2H), 3.40 (t, 4H), 4.39 (t, 2H), 6.85 (dd, J = 8.80, 2.20 Hz, 1H), 6.97 (d, J = 2.20 Hz, 1H), 7.71 (m, 2H), 8.17 (d, J = 8.80 Hz, 1H), 8.22 (d, J = 8.80 Hz, 2H), 8.44 (d, J = 8.80 Hz, 2H), 8.62 (d, J = 7.08 Hz, 1H), 8.71 (dd, J = 7.60, 1.20 Hz, 1H); ^{13}C NMR (100 MHz, [D_3]chloroform, TMS): δ = 13.79, 14.04, 19.29, 20.38, 29.34, 30.77, 51.34, 65.20, 94.13, 109.44, 113.30, 118.70, 122.04, 123.37, 123,38, 123.59, 124.19, 125.16, 126.14, 126.29, 127.00, 130.09, 131.04, 132.20, 137.15, 138.06, 147.88, 159.06, 160.42, 166.04; IR (KBr): ν = 1713 cm^{-1}; elemental analysis calcd (%) for $C_{36}H_{38}N_2O_4$: C 76.84, H 6.81, N 4.98; found: C 77.14, H 6.97, N 5.10.

Compound **5a:** M.p. 172.1 °C; ^{1}H NMR (400 MHz, [D_3]chloroform, TMS): δ = 1.02 (m, 9H), 1.43 (tq, J = 7.32 Hz, 4H), 1.53 (tq, J = 7.32 Hz, 2H), 1.66 (tt, J = 7.32 Hz, 4H), 1.81 (tt, J = 6.60 Hz, 2H), 3.40 (t, J = 7.32 Hz, 4H), 4.39 (t, J = 6.60 Hz, 2H), 6.85 (dd, J = 8.80, 2.20 Hz, 1H), 7.00 (d, J = 2.20 Hz, 1H), 7.66 (dd, J = 8.00 Hz, 1H), 7.72 (dd, J = 8.00 Hz, 1H), 8.15 (d, J = 8.00 Hz, 1H), 8.23 (d, J = 8.00 Hz, 2H), 8.43 (d, J = 8.00 Hz, 1H), 8.48 (d, J = 8.00 Hz, 2H), 8.63 (d, J = 8.00 Hz, 1H); ^{13}C NMR (100 MHz, [D_3]chloroform, TMS): δ = 13.79, 14.03, 19.29, 20.38, 29.32, 30.76, 51.34, 65.21, 94.59, 109.18, 113.37, 116.50, 117.46, 121.39, 121.57, 124.42, 124.80, 126.43, 126.52, 127.18, 127.62, 130.08, 130.95, 132.50, 143.66, 146.41, 147.51, 158.80, 161.73, 165.98; IR (KBr): ν = 1719 cm^{-1}; elemental analysis calcd (%) for $C_{36}H_{38}N_2O_4$: C 76.84, H 6.81, N 4.98; found: C 76.72, H 6.80, N 4.99.

2-[4-(2,3,4,5,6-pentafluorobenzoxy) carbonylphenyl]-10-dibutylamino-benzofuro[2,3-*e*]naphth[1,2-*d*]oxazole **(4b)**: A solution of the mixture of 4a' and 5a' (2.00 g, 3.95 mmol), pentafluorobenzyl bromide (1.93 g, 7.40 mmol), and Na_2CO_3 (0.99 g, 9.38 mmol) in DMF (15 mL) was stirred at 100 °C for 4 h. The reaction mixture poured into cold water, causing the precipitate and then filtered. The resulting residue was extracted with CH_2Cl_2, and washed with water. The organic extract was evaporated. The residue was chromatographed on silica gel (CH_2Cl_2 as eluent) to give 4b (2.02 g, yield 75%) as a yellow powder.

Compound **4b:** M.p. 191.2 °C; ^{1}H NMR (400 MHz, [D_3]chloroform, TMS): δ = 1.01 (t, J = 8.00 Hz, 6H), 1.44 (tq, J = 8.00 Hz, 4H), 1.68 (tt, J = 8.00 Hz, 4H), 3.41 (t, J = 8.00 Hz, 4H), 5.51 (s, 2H), 6.86 (dd, J = 8.80, 2.40 Hz, 1H), 6.97 (d, J = 2.40 Hz, 1H), 7.71 (m, 2H), 8.19 (d, J = 8.00 Hz, 2H), 8.44 (d, J = 8.00 Hz, 2H), 8.62 (d, J = 8.80 Hz, 1H), 8.71 (d, J = 8.80 Hz, 1H); ^{13}C NMR (100 MHz, [D_3]chloroform, TMS): δ = 14.03, 20.39, 29.34, 51.34, 94.11, 109.48, 113.25, 118.86, 122.06, 123.36, 123.59, 123.60, 124.20, 124.22, 125.21, 125.22, 126.20, 126.31, 127.08, 130.33, 130.34, 130.74, 131.63, 131.64, 135.74, 137.13, 137.99, 147.93, 159.09, 160.13, 165.24; IR (KBr): ν = 1720 cm^{-1}; elemental analysis calcd (%) for $C_{39}H_{31}N_2O_4F_5$: C 68.22, H 4.55, N 4.08; found: C 68.26, H 4.76, N 4.02.

2-(9-anthryl)-10-dibutylamino-benzofuro[2,3-*e*]naphth[1,2-*d*] oxazole **(4c)** and 2-(9-anthryl)-10-dibutyl amino-benzofuro[2,3-*e*] naphth[2,1-*d*]oxazole **(5c)**: A solution of 3 (1.00 g, 2.66 mmol), 9-anthraldehyde (0.82 g, 4.00 mmol), and ammonium acetate (4.11 g, 53 mmol) in acetic acid (60 mL) was stirred at 90 °C for 2 h. After concentrating under reduced pressure, the resulting residue was dissolved in CH_2Cl_2, and washed with water. The organic extract was evaporated. The residue was chromatographed on silica gel (xylene : acetic acid = 20 : 1 as eluent) to give 4c (0.46 g, yield 31%) as a red powder and 5c (0.33 g, yield 22%) as an orange powder.

Compound **4c:** M.p. 112–114 °C; ^{1}H NMR (400 MHz, [D_6]acetone, TMS): δ = 1.00 (t, J = 7.32 Hz, 6H), 1.42–1.51 (m, 4H), 1.67–1.75 (m, 4H), 3.51 (t, J = 7.56 Hz, 4H), 7.03 (dd, J = 8.80, 1.70 Hz, 1H), 7.09 (d, J = 2.20 Hz, 1H), 7.63–7.67 (m, 4H), 7.78–7.87 (m, 2H), 8.27–8.30 (m, 4H), 8.40 (d, J = 8.80 Hz, 1H), 8.76 (d, J = 8.04 Hz, 1H), 8.86 (d, J = 8.56 Hz, 1H), 8.95 (s, 1H); ^{13}C NMR (100 MHz, [D_3]chloroform, TMS): δ = 14.03, 20.38, 29.35, 51.33, 94.29, 109.46, 113.44, 118.33, 121.24, 122.08, 123.54, 123.72, 124.22, 125.19, 125.55, 125.75, 126.09, 126.30, 127.39, 128.64, 130.76, 131.15, 131.66, 136.21, 136.74, 138.46, 147.86, 159.07, 160.23; IR (KBr): ν = 1506, 1632 cm^{-1}; elemental analysis calcd (%) for $C_{39}H_{34}N_2O_2$: C 83.24, H 6.09, N 4.98; found: C 83.21, H 6.13, N 4.85.

Compound **5c:** M.p. 174–176 °C; ^{1}H NMR (400 MHz, [D_6]acetone, TMS): δ = 1.02 (t, J = 7.32 Hz, 6H), 1.43–1.55 (m, 4H), 1.69–1.77 (m, 4H), 3.52 (t, J = 7.56 Hz, 4H), 7.02 (dd, J = 8.80, 2.44 Hz, 1H), 7.14 (d, J = 2.20 Hz 1H), 7.63–7.67 (m, 4H), 7.72–7.76 (m, 1H), 7.83–7.87 (m, 1H), 8.25–8.30 (m, 4H), 8.38 (d, J = 9.04 Hz, 1H), 8.44 (d, J = 8.04 Hz, 1H), 8.87 (d, J = 8.32 Hz, 1H), 8.96 (s, 1H); ^{13}C NMR (100 MHz, [D_3] chloroform, TMS): δ = 14.04, 20.40, 29.37, 51.36, 94.77, 109.24, 113.60, 116.40, 117.68, 121.32, 121.64, 124.42, 124.81, 125.57, 125.58, 125.81, 125.82, 126.34, 126.50, 127.37, 128.62, 130.83, 131.13, 131.57, 144.05, 146.92, 147.54, 158.89, 161.67; IR (KBr): ν = 1507, 1634 cm^{-1}; elemental analysis calcd (%) for $C_{39}H_{34}N_2O_2$: C 83.24, H 6.09, N 4.98; found: C 83.41, H 6.19, N 4.87.

1-(1-pyrenyl)-10-dibutylamino-benzofuro[2,3-*e*]naphth[1,2-*d*] oxazole **(4d)** and 2-(1-pyrenyl)-10-dibutyl amino-benzofuro[2,3-*e*] naphth[2,1-*d*]oxazole **(5d)**: A solution of 3 (1.00 g, 2.66 mmol),

Table 1
Spectroscopic data of **4a**–**4f** and **5a**, **5c**–**5d** in 1,4-dioxane and in the solid state.

Compound	In 1,4-dioxane		In the solid state	
	λ_{max}^{abs}/nm (ε_{max}/dm^3 mol^{-1} cm^{-1})	λ_{max}^{fl}/nm (Φ)	λ_{max}^{ex}/nm	λ_{max}^{em}/nm (Φ)
4a	413 (28900), 360 (17700)	518 (0.82)	539	578 (0.11)
4b	420 (31000), 360 (16000)	535 (0.81)	555	605 (0.49)
4c	408 (16000), 371 (27000)	569 (0.60)	547	602 (0.07)
4d	436 (32700), 398 (27100)	536 (0.83)	528	570 (0.02)
4e	[a]410^{sh}, 392 (38000)	460 (0.83)	458	490 (0.43)
4f	388 (36100)	448 (0.86)	453	486 (0.63)
5a	367 (30400)	546 (0.28)	534	573 (0.11)
5c	410 (4000), 372 (298000)	571 (0.12)	510	564 (0.03)
5d	416 (168000), 396 (34000), 376 (46200)	550 (0.43)	508	564 (0.07)

[a] Shoulder absorption.

1-pyrencarbaldehyde (0.92 g, 4.00 mmol), and ammonium acetate (4.11 g, 53 mmol) in acetic acid (60 mL) was stirred at 90 °C for 2 h. After concentrating under reduced pressure, the resulting residue was dissolved in CH_2Cl_2, and washed with water. The organic extract was evaporated. The residue was chromatographed on silica gel (xylene : acetic acid = 20 : 1 as eluent) to give 4d (0.77 g, yield 49%) as an orange powder and 5d (0.56 g, yield 36%) as a yellow powder.

Compound **4d:** M.p. 222–224 °C; ^{1}H NMR (400 MHz, [D$_6$]acetone, TMS): δ = 1.04 (t, J = 7.32 Hz, 6H), 1.45–1.54 (m, 4H), 1.70–1.78 (m, 4H), 3.53 (t, J = 7.32 Hz, 4H), 7.02 (dd, J = 8.80, 2.44 Hz, 1H), 7.12 (d, J = 2.44 Hz, 1H), 7.82–7.84 (m, 2H), 8.17–8.22 (m, 1H), 8.29–8.38 (m, 3H), 8.42–8.47 (m, 2H), 8.51–8.55 (m, 2H), 8.80–8.82 (m, 1H), 8.84–8.87 (m, 1H), 9.11 (d, J = 8.32 Hz, 1H), 10.15 (d, J = 9.52 Hz, 1H); ^{13}C NMR (100 MHz, [D$_3$]chloroform, TMS): δ = 14.07, 20.42, 29.38, 51.34, 94.20, 109.28, 113.51, 118.04, 120.04, 121.92, 123.53, 123.60, 123.61, 124.09, 124.28, 124.29, 124.64, 124.85, 125.00, 125.65, 125.66, 125.81, 125.84, 125.95, 126.15, 127.15, 127.18, 128.90, 128.91, 129.36, 129.37, 130.63, 131.15, 133.00, 137.55, 138.22, 147.67, 158.93, 161.68; IR (KBr): ν = 1506, 1635 cm^{-1}; elemental analysis calcd (%) for $C_{41}H_{34}N_2O_2$: C 83.93, H 5.84, N 4.77; found: C 84.11, H 5.84, N 4.64.

Table 2
Calculated absorption spectra for the compounds **4a**–**4f** and **5a, 5c**–**5d**.

	μ/D[a]	Absorption (calc.)		CI component[c]	$\Delta\mu$/D[d]
		λ_{max}/nm	f[b]		
4a	5.35	427	1.02	HOMO→LUMO(79%)	11.76
				HOMO→LUMO(79%)	
4b	5.09	430	1.04	HOMO→LUMO+1(10%)	12.36
		390	0.97	HOMO→LUMO+1(53%)	
4c	2.31			HOMO→LUMO(30%)	4.94
		343	0.12	HOMO−1→LUMO(42%)	
4d	2.04	416	1.36	HOMO→LUMO(62%)	7.09
		341	0.10	HOMO→LUMO+1(35%)	
4e	4.09	413	0.99	HOMO→LUMO(87%)	
		357	0.09	HOMO→LUMO+3(41%)	7.55
4f	2.31	407	1.02	HOMO→LUMO(89%)	
		314	0.64	HOMO→LUMO+1(38%)	6.58
		399	0.30	HOMO→LUMO(62%)	
5a	3.44	353	0.32	HOMO→LUMO+1(71%)	13.00
		343	1.01	HOMO-1→LUMO(28%)	
		366	0.14	HOMO→LUMO+2(56%)	
				HOMO→LUMO(12%)	
5c	1.68	352	0.89	HOMO→LUMO+1(74%)	3.81
		349	0.19	HOMO-1→LUMO(50%)	
		381	0.47	HOMO→LUMO(40%)	
5d	1.63	354	0.26	HOMO-1→LUMO(34%)	7.37
		351	1.12	HOMO→LUMO+1(75%)	

[a] The values of the dipole moment in the ground state.
[b] Oscillator strength.
[c] The transition is shown by an arrow from one orbital to another, followed by its percentage CI (configuration interaction) component.
[d] The difference in the dipole moment between the excited and the ground states.

Compound **5d:** M.p. 174–176 °C; ^{1}H NMR (400 MHz, [D$_6$]acetone, TMS): δ = 1.04 (t, J = 7.56 Hz, 6H), 1.48–1.53 (m, 4H), 1.71–1.79 (m, 4H), 3.53 (t, J = 7.56 Hz, 4H), 7.01 (dd, J = 8.76, 2.44 Hz, 1H), 7.18 (d, J = 1.92 Hz, 1H), 7.78–7.87 (m, 2H), 8.18–8.22 (m, 1H), 8.31–8.39 (m, 3H), 8.43–8.49 (m, 2H), 8.53–8.57 (m, 2H), 8.64–8.67 (m, 1H), 8.84–8.86 (m, 1H), 9.21 (d, J = 8.28 Hz, 1H), 10.18 (d, J = 9.52 Hz, 1H); ^{13}C NMR (100 MHz, [D$_3$]chloroform, TMS): δ = 14.07, 20.42, 29.38, 51.39, 94.67, 109.05, 113.60, 116.13, 117.37, 119.97, 121.44, 121.51, 124.22, 124.28, 124.55, 124.57, 124.95, 125.68, 125.69, 125.94, 126.01, 126.13, 126.18, 127.13, 127.35, 127.82, 129.06, 129.47, 129.52, 130.60, 131.11, 133.19, 143.84, 145.72, 147.35, 158.68, 163.10; IR (KBr): ν = 1507, 1634 cm^{-1}; elemental analysis calcd (%) for $C_{41}H_{34}N_2O_2$: C 83.93, H 5.84, N 4.77; found: C 84.08, H 5.73, N 4.70.

Table 3
Crystal data and structure refinement parameters for the compounds **4c** and **5c**.

Compound	4c	5c
Molecular formula	$C_{39}H_{34}N_2O_2$	$C_{39}H_{34}N_2O_2$
Formula weight	562.71	562.71
Crystal size[nm]	0.40 × 0.10 × 0.40	0.60 × 0.40 × 0.50
Reflns[a] (2θ range, [°])	23 (22.3–24.0)	25 (27.0–29.6)
Crystal system	Monoclinic	Monoclinic
Space group	P2$_1$/n	P2$_1$/n
a [Å]	13.267(3)	15.127(2)
b [Å]	11.975(2)	9.553(1)
c [Å]	19.782(3)	21.941(2)
β [°]	107.13(1)	108.461(7)
V [Å^3]	3003.6(8)	3007.5(6)
Z	4	4
ρ_{calcd} [g cm^{-3}]	1.244	1.243
F(000)	1192.0	1192.0
μ(Mo$_{k\alpha}$) [cm^{-1}]	0.76	0.76
T [K]	296.2	296.2
Scan mode	ω–2θ	ω–2θ
Scan rate [ω min^{-1}]	8.0[b]	8.0[b]
Scan width [°]	1.52 + 0.30	1.68 + 0.30
2θ max [°]	tanθ	tanθ
hkl range	50.0	50.0
	0/15	0/17
	−14/0	0/11
Reflns measured	−23/22	−26/24
Unique reflns	5819	5864
Reflns observed with $I_0 > 2\sigma I_0$	5492	5287
R_{int}	1341	2954
No. of parameters	0.135	0.018
R	453	513
Rw	0.0667	0.050
W	0.1194	0.1130
S	$(\sigma^2F^2)^{-1}$	$(\sigma^2F^2)^{-1}$
Max. shift/error in final cycle	0.95	1.26
Max. peak in final diff. Map	0.01	0.01
[e Å^{-3}]	0.35	0.23
Min. peak in final diff. Map		
[e Å^{-3}]	−0.40	−0.18

[a] Number of reflections used for unit cell determination.
[b] Up to five scans.

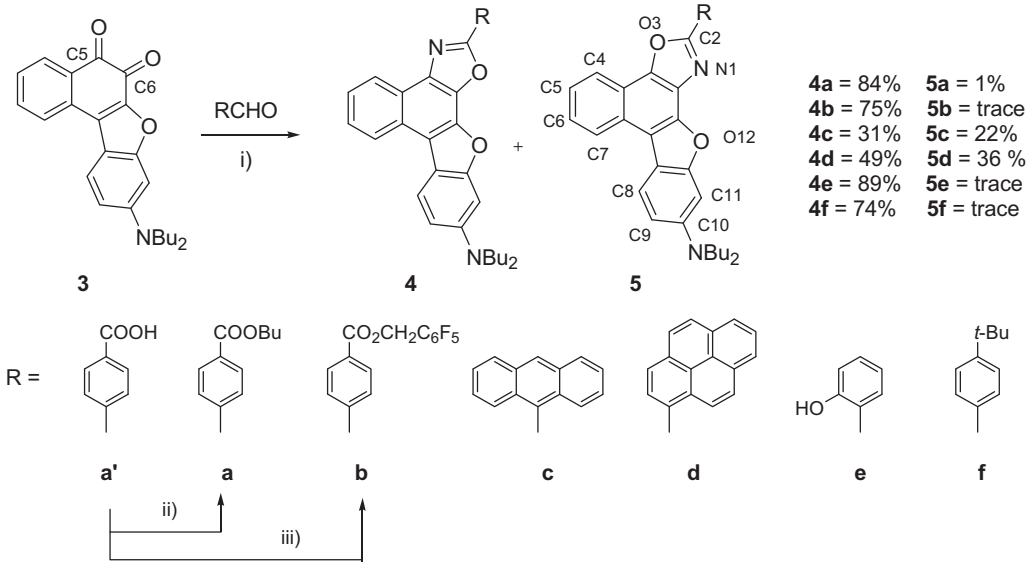

Scheme 1. Synthesis of fluorophores **4** and **5**. i) CH_3COOH, CH_3COONH_4, 90 °C, 1–5 h; ii) BuI, Na_2CO_3, DMF, 100 °C, 10 h; iii) pentafluorobenzyl bromide, Na_2CO_3, DMF, 100 °C, 4 h.

2-(2-hydroxylphenyl)-10-dibutylamino-benzofuro[2,3-*e*] naphth[1,2-*d*]oxazole (4e): A solution of **3** (1.00 g, 2.66 mmol), salicylaldehyde (0.39 g, 3.22 mmol), and ammonium acetate (4.11 g, 53 mmol) in acetic acid (30 mL) was stirred at 90 °C for 5 h. The reaction mixture poured into cold water, causing the precipitate and then filtered. The residue was dissolved in CH_2Cl_2, and washed with water. The organic extract was evaporated. The residue was chromatographed on silica gel (CH_2Cl_2 as eluent) to give **4e** (1.13 g, yield 89%) as a yellow powder.

Compound **4e:** M.p. 184.3 °C; ^{1}H NMR (400 MHz, [D_3]chloroform, TMS): δ = 1.01 (t, 6H), 1.39–1.49 (m, 4H), 1.65–1.72 (m, 4H), 3.39 (t, 4H), 6.86 (dd, J = 8.80, 2.44 Hz, 1H), 6.99(d, J = 2.44 Hz 1H), 7.05–7.09 (m, 1H), 7.18 (d, J = 8.08 Hz 1H), 7.44–7.48 (m, 1H), 7.67–7.75 (m, 2H), 8.16–8.19 (m, 2H), 8.58–8.63 (m, 2H), 11.48 (s, 1H); ^{13}C NMR (100 MHz, [D_3]chloroform, TMS): δ = 14.03, 20.38, 29.35, 51.32, 94.00, 109.34, 110.89, 113.07, 117.25, 118.42, 119.66, 121.88, 122.41, 123.08, 124.09, 125.05, 126.09, 126.10, 126.65, 132.91, 133.68, 134.67, 137.76, 147.81, 157.95, 158.89, 160.97; IR (KBr): ν = 3059 cm^{-1}; elemental analysis calcd (%) for $C_{31}H_{30}N_2O_3$: C 77.80, H 6.32, N 5.85; found: C 77.93, H 6.41, N 6.02.

2-(4-tert-butylphenyl)-10-dibutylamino-benzofuro[2,3-*e*] naphth[1,2-*d*]oxazole (4f): A solution of **3** (1.00 g, 2.66 mmol), 4-tert-butyl-benzaldehyde (0.52 g, 3.20 mmol), and ammonium acetate (4.10 g, 53 mmol) in acetic acid (20 mL) was stirred at 90 °C for 1 h. The reaction mixture poured into cold water, causing the precipitate and then filtered. The residue was dissolved in CH_2Cl_2, and washed with water. The organic extract was evaporated. The residue was chromatographed on silica gel (CH_2Cl_2 as eluent) to give **4f** (1.00 g, yield 74%) as a yellow powder.

Compound **4f:** M.p. 220–221 °C; ^{1}H NMR (400 MHz, [D_3]chloroform, TMS): δ = 1.01 (t, 6H), 1.38 (s, 9H), 1.39–1.47 (m, 4H), 1.64–1.71 (m, 4H), 3.40 (t, 4H), 6.85 (dd, J = 8.80, 2.44 Hz, 1H), 6.98 (d, J = 2.44 Hz, 1H), 7.58 (d, J = 8.80 Hz, 2H), 7.65–7.72 (m, 2H), 8.17 (d, J = 8.80 Hz, 1H), 8.31 (d, J = 8.56 Hz, 2H), 8.58 (d, J = 7.60 Hz, 1H), 8.72 (d, J = 7.60 Hz, 1H); ^{13}C NMR (100 MHz, [D_3]chloroform, TMS): δ = 14.04, 20.40, 29.36, 31.19, 35.05, 51.37, 94.26, 109.34, 113.05, 117.82, 121.92, 123.44, 123.56, 124.11, 124.56, 124.86, 125.86, 125.91, 126.16, 127.12, 135.28, 137.28, 138.39, 147.70, 154.48, 158.90, 161.83; IR (KBr): ν = 1635 cm^{-1}; elemental analysis calcd (%) for $C_{35}H_{38}N_2O_2$: C 81.05, H 7.38, N 5.40; found: C 80.80, H 7.50, N 5.42.

2.1. X-ray crystallographic studies

The reflection data were collected at 23 ± 1 °C on a Rigaku AFC7S four-circle diffractometer by 2θ–ω scan technique, and using graphite-monochromated $Mo_{K\alpha}$ (λ = 0.71069 Å) radiation at 50 kV

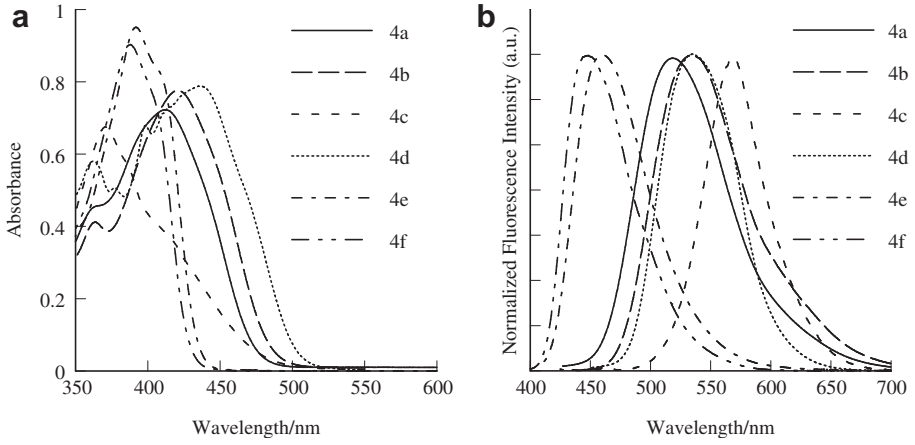

Fig. 2. a) Absorption and b) fluorescence spectra of the compounds **4a**–**4f** in 1,4-dioxane.

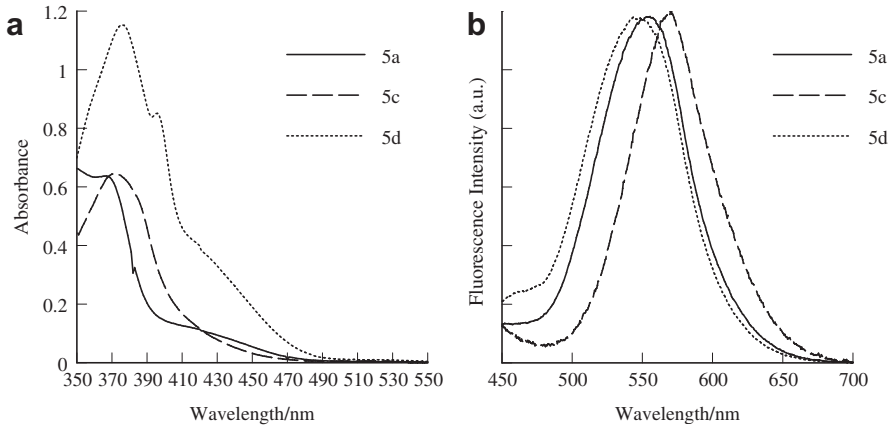

Fig. 3. a) Absorption and b) fluorescence spectra of the compounds **5a**, **5c** and **5d** in 1,4-dioxane.

and 30 mA. In all cases, the data were corrected for Lorentz and polarization effects. A correction for secondary extinction was applied. The reflection intensities were monitored by three standard reflections for every 150 reflections. An empirical absorption correction based on azimuthal scans of several reflections was applied. All calculations were performed using the teXsan [19] crystallographic software package of Molecular Structure Corporation. CCDC-797585 (**4c**) and CCDC-797586 (**5c**) contain the supplementary crystallographic data (see Table 3) for this paper. These data can be obtained free of charge from The Cambridge Crystallographic Data Centre via www.ccdc.cam.au.uk/data_request/cif.

Compound **4c:** Crystals of **4c** were recrystallized from ethanol to afford air stable yellow prism. The transmission factors ranged from 0.96 to 1.00. The crystal structure was solved by direct methods using SIR 92 [20]. The structures were expanded using Fourier techniques [21]. The non-hydrogen atoms were refined anisotropically. Some hydrogen atoms were refined isotropically, the rest were fixed geometrically and not refined.

Compound **5c:** Crystals of **5c** were recrystallized from ethanol to afford air stable yellow prism. The transmission factors ranged from 0.94 to 1.00. The crystal structure was solved by direct methods using SIR 92 [20]. The structures were expanded using Fourier techniques [21]. The non-hydrogen atoms were refined anisotropically. Some hydrogen atoms were refined isotropically, the rest were fixed geometrically and not refined.

3. Result and discussion

The synthetic pathway is shown in Scheme 1. Quinone **3** [18] was allowed to react with various arylaldehydes in the presence of ammonium acetate to give the benzofuro[2,3-*e*]naphthoxazole-type fluorophores **4** and **5**. The isomers **4** were preferentially obtained in each case. In this reaction, NH_3 resulting from ammonium acetate in the initial stage acts as the nucleophilic reagent to the 5- and/or 6-carbonyl carbon. In this case, NH_3 preferentially attacks the 5-carbonyl carbon rather than the 6-carbonyl in spite of the similar steric reactivity of the two carbonyls. It was considered that the conjugated linkage of the dibutylamino group to the 6-carbonyl group would make the 6-carbonyl carbon less electrophilic than the 5-carbonyl carbon, so that the nucleophilic reagents (NH_3) preferentially attack the electrophilic 5-carbonyl carbon. As a result of these features this reaction afforded preferentially compounds **4**. Moreover, the yields of the isomers **5** were increased when the bulky aldehydes such as 9-anthraldehyde and 1-pyrenylcarbaldehyde were used as the reagent. It was considered that the reaction of the aldehyde with the resulting 5-imine group resulted in steric hindrance between the substituent of aldehyde and hydrogen atom

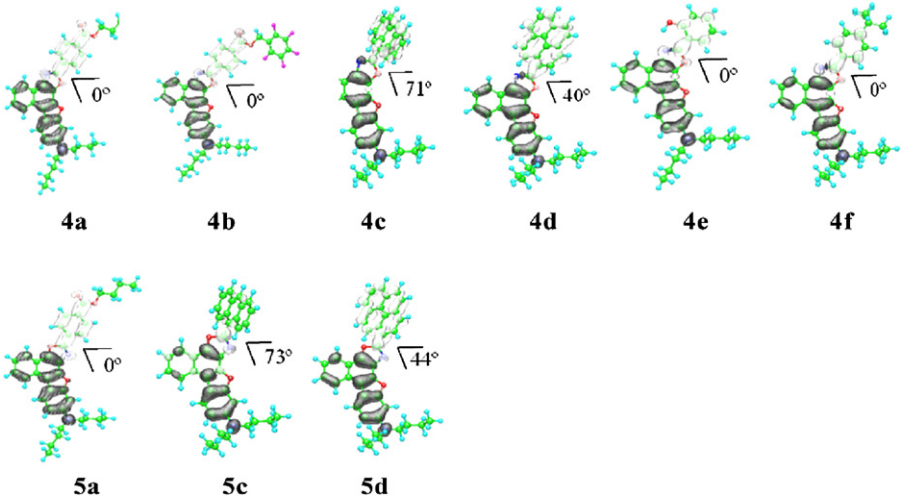

Fig. 4. Calculated changes in electron density accompanying the first electronic excitation of **4a**–**4f**, **5a**, and **5c**–**5d**. The black and white lobes signify degreases and increase in electron density accompanying the electronic transition, respectively. Their areas indicate the magnitude of the electron density change.

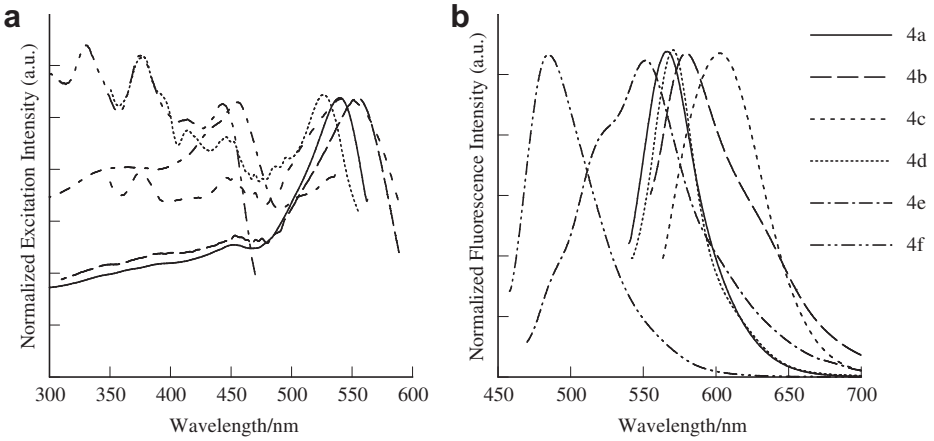

Fig. 5. a) Excitation and b) emission spectra of the compounds **4a**–**4f** in the solid state.

of adjacent benzen ring. These compounds were completely characterized by ^{1}H, ^{13}C NMR, IR, and elemental analysis. A comparison of the observed and calculated UV–VIS spectra for compounds **4** and **5** have provided a powerful evidence for identification of their structures, which will be described later on.

The absorption and fluorescence spectral data of **4a**–**4f** and **5a**, **5c**–**5d** in solution are summarized in Table 1 and their spectra in 1,4-dioxane are shown in Figs. 1 and 2, respectively. The visible absorption and fluorescence intensities of **4** are much stronger than those of **5** in 1,4-dioxane. The fluorophores **4a**–**4d** showed two absorption bands at around 408–436 and 360–398 nm and a single intense fluorescence band at around 518–569 nm in 1,4-dioxane. The fluorophores **4e** and **4f** exhibited an intense absorption band at around 388–392 nm and a single intense fluorescence band at around 448–460 nm in 1,4-dioxane. The fluorescence quantum yields (Φ) of the fluorophores **4** were 0.82–0.88 expect for **4c**. On the other hand, the fluorophores **5** exhibit an intense absorption band at around 366–396 nm, and a relatively weak fluorescence band at around 550–571 nm ($\Phi = 0.12$–0.43) in 1,4-dioxane (Fig. 3). The Φ values of **4** greater than those of **5** suggest that the degree of donor–acceptor conjugation for the former is larger than that for the latter owing to the conjugated linkage of the dibutylamino group to the 6-substituents in **4**.

The photophysical spectra of **4** and **5** were analyzed by using semi-empirical molecular orbital (MO) calculations. The molecular structures were optimized by using MOPAC/AM1 method [22], and then the INDO/S method [23,24] was used for spectroscopic calculations. The calculated absorption wavelengths and the transition character of the first absorption bands are collected in Table 2. The calculated absorption wavelengths and the oscillator strength values compare favourably with the observed spectra in 1,4-dioxane, although the calculated absorption spectra are blue-shifted. This deviation of the INDO/S calculations, giving high transition energies compared with the experimental values, has been generally observed [25,26]. The calculations indicate that the longest excitation bands for both isomers **4** and **5** are mainly assignable to the transition from the HOMO to the LUMO, where HOMO is mostly localized on the 10-dibutylamino-benzofuro[2,3-*e*]naphthoxazole moiety and the LUMO is mostly localized on the substituent moiety (R). The changes in the calculated electron density accompanying the first electron excitation are shown in Fig. 4, which reveal a strong migration of intramolecular charge transfer from the 10-dibutylamino-benzofuro[2,3-*e*]naphthoxazole moiety to the substituent moiety (R) in all the dyes except for **5c**. In the longest excitation bands, the oscillator strengths (*f*) of isomers **4** are rather larger than those of isomers **5**, which is also in good agreement with the experimental data. The calculations reveal that a strong migration of intramolecular charge transfer from the donor moiety to the acceptor moiety for **4a**–**4e** with the conjugated linkage of the dibutylamino group to the substituents leads to intense visible absorption and fluorescence properties. In addition, in the dye **5c**, the calculated electron density changes accompanying the first electron excitation show mainly within the benzofuronaphthoxazole moiety. This result is attributed to decrease of the donor–acceptor conjugation arising from steric hindrance between 10-dibutylamino-benzofuro[2,3-*e*]naphthoxazole plane

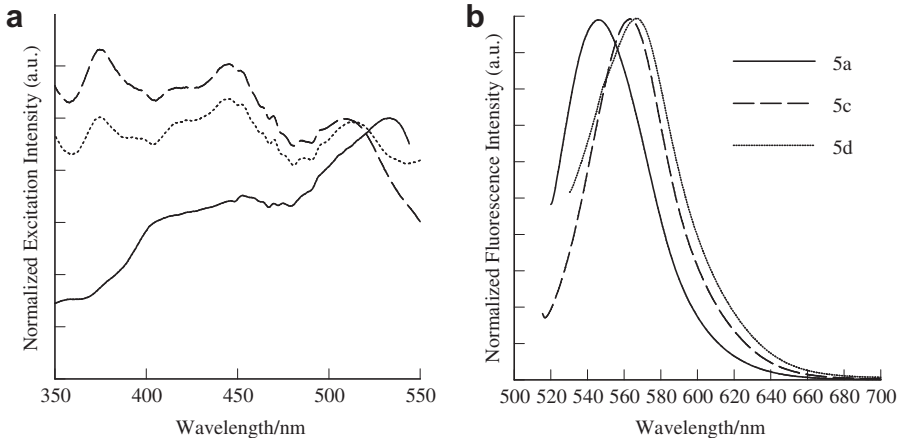

Fig. 6. a) Excitation and b) emission spectra of the compounds **5a**, **5c**–**5d** in the solid state.

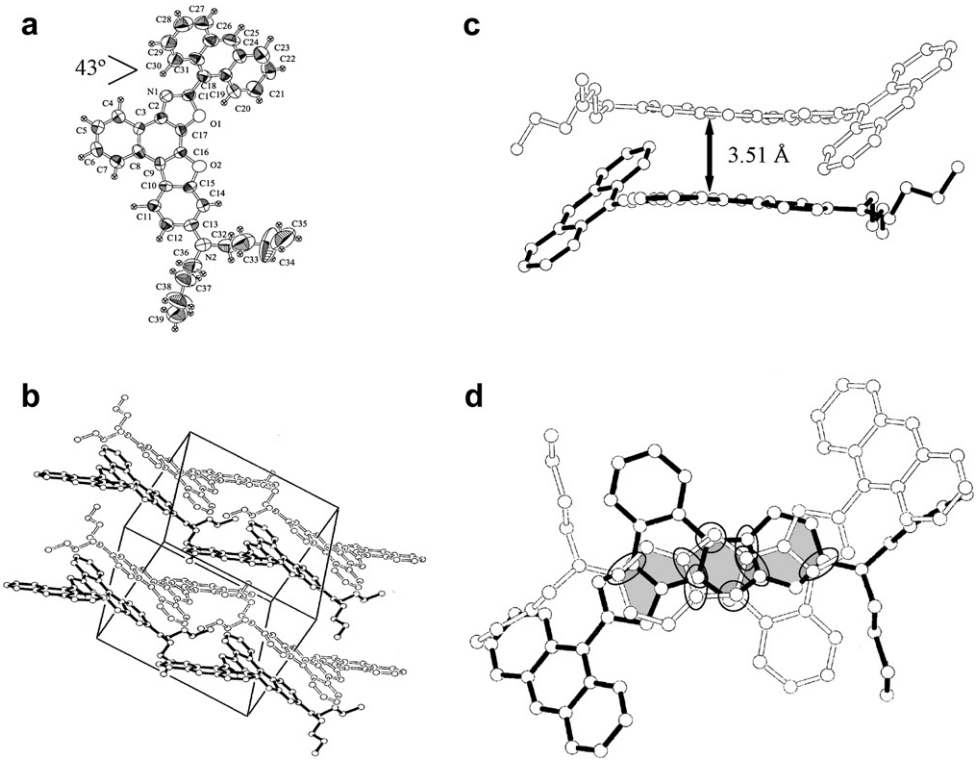

Fig. 7. Crystal packing of **4c** (a) a schematic structure, (b) a stereoview of the molecular packing structure, (c) a side view, and (d) a top view of the pairs of fluorophores.

and the anthranyl group. On the other, hand, the longest excitation band of **4f** were blue-shifted by 17 nm compared to that of **4a**. It can also explain that the degree of donor–acceptor conjugation of **4f** is lower because of the weaker acceptor group.

Figs. 5 and 6 and Table 1 show the spectroscopic properties of the crystals of the fluorophores **4** and **5**. Many remarkable differences are seen when the absorption and fluorescence spectra in the solid state are compared to those in solution. The wavelength of the fluorescence excitation and emission maxima of **4** are largely red-shifted compared with those in 1,4-dioxane. On the other hand, the fluorescence excitation wavelengths of **5** are also largely red-sifted compared with those in 1,4-dioxane. The fluorescence wavelengths of **5** are red-shifted for **5a** and **5d** and are blue-shifted for **5c** compared with those in 1,4-dioxane, respectively.

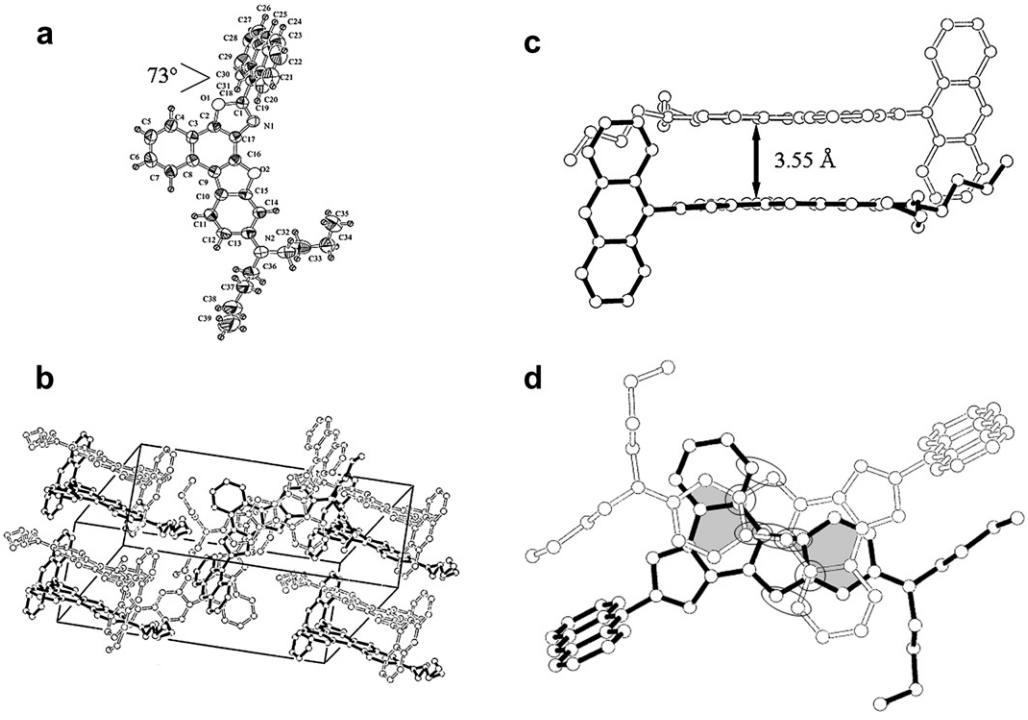

Fig. 8. Crystal packing of **5c** (a) a schematic structure, (b) a stereoview of the molecular packing structure, (c) a side view, and (d) a top view of the pairs of fluorophores.

Furthermore, it was found that the fluorophores **4b**, **4e** and **4f** exhibited strong emission even in the solid state. Generally, the fluorescence in the solid state was strongly quenched by intense π–π interactions. This result shows that the fluorescence of **4a**, **4c**, **4d**. **5a**, **5c** and **5d** was strongly quenched by strong π–π interactions, but the fluorescence of **4b**, **4e** and **4f** which have the bulky substituent was not so strongly quenched by π–π interactions.

In order to investigate the above hypothesis, we performed X-ray crystallographic analysis of **4c** and **5c**. The packing structures demonstrate that the molecules are arranged in a "herring-bone" fashion in the crystal of **4c** (Fig. 7(b)), and in a "bricks in a wall" fashion in the crystal of **5c** (Fig. 8(a)), respectively. The anthranyl group of **4c** is twisted out of the plane of the naphthoxazole skeleton by 43° (Fig. 7(a)). The interplanar distance between the oxazole plates is ca. 3.51 Å and there are 8 short interatomic π–π contacts within the pair of fluorescent dyes, which suggests strong π–π interactions. On the other hand, the anthranyl group of **5c** is twisted out of the plane of the naphthoxazole skeleton by 73° (Fig. 8(a)), which is large compared to the torsion angle of **4c**. As shown in Fig. 8(c), the interplanar distance between the oxazole plates is ca. 3.55 Å, which is longer in comparison with the dye **4c** and there are 7 short interatomic π–π contacts between the pair of fluorescent dyes. A strong intermolecular π–π interaction between neighbouring fluorophores is a principal factor of the large red-shift of the absorption and fluorescence maxima and an intense fluorescence quenching in the solid state [18,27–31]. Consequently, the fluorescence of these dyes was strongly quenched by strong π–π interactions in the solid state.

4. Conclusion

We have synthesized and characterized novel benzofuro[2,3-*e*] naphthoxazole-type isomeric fluorophores **4a**–**4f** and **5a**, **5c**–**5d**. It was found that the main products were isomers **4** whose absorption and fluorescence intensities are much stronger than the isomers **5**. In solution, the fluorescence quantum yields of the fluorophores **4** were 0.60–0.86, whereas those of the isomers **5** were 0.12–0.43. In the solid state, both fluorophores **4** and **5** generally exhibited longer absorption and fluorescence wavelengths and lower quantum yields in comparison with those in solution. For example, the fluorescence quantum yields of **4c** and **4d** exhibited small values ($\Phi = 0.02$–0.07) because of the strong π–π interactions. However, the fluorophores **4b**, **4e**, and **4f** which have bulky substituent exhibited strong emission ($\Phi = 0.43$–0.63) due to the reduction of π–π interactions.

Acknowledgments

This work was partially supported by a Grant-in-Aid for Science and Research from the Ministry of Education, Science, Sport and Culture of Japan (Grant 21550181) and by a Adaptable and Seamless Technology Transfer Program through Target-driven R&D of Japan Science and Technology Agency (JST).

References

[1] Kowalski E, Aniliker R, Schmid K. Performance parameters of some new efficient and highly soluble solutes for liquid scintillators. Mol Crys 1968;4:403.
[2] Cassard P, Corkum PB, Alcock AJ. Solvent dependent characteristics of xenon chloride (XeCl) pumped UV dye lasers. Appl Phys 1981;25:17.
[3] Pla-Dalmau A. 2-(2'-Hydroxyphenyl)benzothiazoles, -benzoxazoles, and -benzimidazoles for plastic scintillation applications. J Org Chem 1995;60: 5468.
[4] Kanegae Y, Peariso K, Martinez SS. Class of photostable, highly efficient UV dyes: 2-phenylbenzoxazoles. Appl Spectrosc 1996;50:316.
[5] Rodriguez AD, Ramirez C, Rodriguez II , González E. Novel antimycobacterial benzoxazole alkaloids, from the West Indian sea whip pseudopterogorgia elisabethae. Org Lett 1999;1:527.
[6] Chen P, Cheng PTW, Alam M, Beter BD, Bisacchi GS, Dejneka T, et al. Of P1/P1' compounds: correlation between lipophilicity and cytotoxicity. J Med Chem 1991;1996:39.
[7] Meyer MD, Hancock AA, Tietje K, Sippy KB, Prasad R, Stout DM, et al. Structure-activity studies for a novel series of dual 5-HT uptake inhibitors/2-antagonists. J Med Chem 1997;40:1049.
[8] Sato Y, Yamada M, Yoshida S, Soneda T, Ishikawa M, Nizato T, et al. Benzoxazole derivatives as novel 5-HT3 receptor partial agonists in the gut. J Med Chem 1998;41:3015.
[9] Reynold MB, Deluca MR, Kerwin SM. The novel bis(benzoxazole) cytotoxic natural product UK-1 is a magnesium ion-dependent DNA binding agent and inhibitor of human topoisomerase II. Bioorg. Chem 1999;27:326.
[10] Tang CW, VansSlyke SA. Organic electroluminescent diodes. Appl Phys Lett 1987;51:913.
[11] Tonzola CJ, Alam MM, Kaminsky WK, Jenekhe SA. New n-type organic semiconductors: synthesis, single crystal structures, cyclic voltammetry, photophysics, electron transport, and electroluminescence of a series of diphenylanthrazolines. J Am Chem Soc 2003;125:13548.
[12] Chiang CL, Wu MF, Dai DC, Wen YS, Wang JK, Chen CT. Red-emitting fluorenes as efficient emitting hosts for non-doped, organic red-light-emitting diodes. Adv Funct Mater 2005;15:231.
[13] Bener D, Klein C, Nazeeruddin MD, de Angelis F, Castellani M, Bugnon P, et al. Efficient blue light-emitting diodes based on a classical "push-pull" architecture molecule 4,4'-di-(2-(2,5-dimethoxyphenyl)ethenyl)-2,2'-bipyridine. J Mater Chem 2006;16:4468.
[14] Thomas KRJ, Kin JT, Hsu YC, Ho KC. Organic dyes containing thienylfluorene conjugation for solar cells. Chem Commun; 2005:4098.
[15] Li SL, Jiang KJ, Shao KF, Yang LM. Novel organic dyes for efficient dye-sensitized solar cells. Chem Commun; 2006:2792.
[16] Ooyama Y, Harima Y. Dramatic effects of the substituents on the solid-state fluorescence properties of structural isomers of novel benzofuro[2,3-c] oxazolocarbazole-type fluorophores. Chem Lett; 2006:902.
[17] Ooyama Y, Kagawa Y, Harima Y. Synthesis and solid-state fluorescence properties of structural isomers of novel benzofuro[2,3-c]oxazolocarbazole-type fluorescent dyes. Eur J Org Chem; 2007:3613.
[18] Ooyama Y, Okamoto T, Yamaguchi T, Suzuki T, Hayashi A, Yoshida K. Heterocyclic quinol-type fluorophores: synthesis, X-ray crystal structures, and solid-state photophysical properties of novel 5-hydroxy-5- substituent-benzo [b]naphtho[1,2-d]furan-6-one and 3-hydroxy-3-substituent- benzo[kl] xanthen-2-one derivatives. Chem Eur J; 2006:7827.
[19] teXsan. Crystal structure analysis package. Molecular Structure Corporation; 1985 and 1992.
[20] Altomare A, Burla MC, Cascarano M, Giacovazzo C, Guagliardi A, Polidori G. *SIR*92-a program for automatic solution of crystal structures by direct methods. J Appl Cryst 1994;27:435.
[21] Beurskens PT, Admiraal G, Beurskens G, Bosman WP, de Gelder R, Israel R, et al, DIRDIF94. The DIRIF94 p.ogram system, technical report of the crystallography laboratory. The Netherlands: University of Nijmegen; 1994.
[22] Dewar MJS, Zoebisch EG, Healy EF, Stewart JJP. Development and use of quantum mechanical molecular models. 76. AM1: a new general purpose quantum mechanical molecular model. J Am Chem Soc 1985;107:3902.
[23] Ridley JE, Zerner MC. Triplet states via intermediate neglect of differential overlap: benzene, pyridine and the diazines. Theor Chim Acta 1976;42:223.
[24] Bacon AD, Zerner MC. An intermediate neglect of differential overlap theory for transition metal complexes: iron, cobalt and copper chlorides. Theor Chim Acta 1979;53:21.
[25] Adachi M, Murata Y, Nakamura S. The relationship between the structures and absorption spectra of cyan color indoaniline dyes. J Org Chem 1993;58:5238.
[26] Fabian WMF, Schuppler S, Wolfbeis OS. Effects of annulation on absorption and fluorescence characteristics of fluorescein derivatives: a computational study. J Chem Soc. Perkin Trans 1996;2:853.
[27] Yeh HC, Wu WC, Wen YS, Dai DC, Wang JK, Chen CT. Derivative of α,β-Dicyanostilbene: convenient Precursor for the synthesis of Diphenylmaleimide compounds, E-ZIsomerization, crystal structure, and solid-state fluorescence. J Org Chem 2004;69:6455.
[28] Mizukami S, Houjou H, Sugaya K, Koyama E, Tokuhisa H, Sasaki T, et al. Fluorescence color modulation by intramolecular and intermolecular pi-pi interactions in a helical zinc(II) complex. Chem Mater 2005;17:50.
[29] Scott JL, Yamada T, Tanaka K. Guest specific solid-state fluorescence rationalised by reference to solid-state structures and specific intermolecular interactions. New J Chem 2004;28:447.
[30] Ooyama Y, Yoshikawa S, Watanabe S, Yoshida K. Molecular design of novel non-planar heteropolycyclic fluorophores with bulky substituents: convenient synthesis and solid-state fluorescence characterization. Org Biomol Chem 2006;4:3406.
[31] Ooyama Y, Yoshida K. Heterocyclic quinol-type fluorophores. Dramatic solid-state fluorescence enhancement behavior of imidazoanthraquinoltype clathrate hosts upon inclusion of various kinds of organic solvent molecules. New J Chem 2005;29:1204.